

- Fleming, K., Johnston, P., Zwartz, D., Yokoyama, Y., Lambeck, K., and Chappell, J. (1998). Refining the eustatic sea-level curve since the Last Glacial Maximum using far- and intermediate-field sites. *Earth and Planetary Science Letters* **163**, 327–342.
- Goodwin, I. D. (2003). Unravelling climatic influences on Late Holocene sea-level variability. In *Global change in the Holocene* (A. Mackay, R. Battarbee, J. Birks and F. Oldfield, Eds.), pp. 406–421. Arnold, London.
- Hanebuth, T., Stategger, K., and Grootes, P. M. (2000). Rapid flooding of the Sunda Shelf: A Late-Glacial sea-level record. *Science* **288**, 1033–1035.
- Lambeck, K. (1995). Late Devensian and Holocene shorelines of the British Isles and North Sea from models of glacio-hydro-isostatic rebound. *Journal of the Geological Society, London* **152**, 437–448.
- Lambeck, K., and Johnston, P. (1995). Land subsidence and sea-level change: Contributions from the melting of the last great ice sheets and the isostatic adjustment of the Earth. In *Land Subsidence* (F. B. J. Barends, F. J. J. Brouwer and F. H. Schröder, Eds.), pp. 3–18. Balkema, Rotterdam.
- Milne, G. A., and Mitrovića, J. X. (1998). Postglacial sea-level change on a rotating Earth. *Geophysical Journal International* **133**, 1–19.
- Mitrovića, J. X., and Milne, G. A. (2002). On the origin of late Holocene sea-level highstands within equatorial ocean basins. *Quaternary Science Reviews* **21**, 2179–2190.
- Murray-Wallace, C. V. (2002). Pleistocene coastal stratigraphy, sea-level highstands and neotectonism of the southern Australian passive continental margin – a review. *Journal of Quaternary Science* **17**, 469–489.
- Murray-Wallace, C. V., Ferland, M. A., and Roy, P. S. (2005). Further amino acid racemisation evidence for glacial age, multiple lowstand deposition on the New South Wales outer continental shelf, southeastern Australia. *Marine Geology* **214**, 235–250.
- Nakada, M., and Lambeck, K. (1989). Late Pleistocene and Holocene sea-level change in the Australian region and mantle rheology. *Geophysical Journal* **96**, 497–517.
- Oppenheimer, S. (1998). *Eden in the East – The drowned continent of southeast Asia*, p. 560. Weidenfeld and Nicolson, London.
- Peltier, W. R. (1998). Global glacial isostatic adjustment and coastal tectonics. In *Coastal Tectonics* (I. S. Stewart and C. Vita-Finzi, Eds.), Vol. 146, pp. 1–29. Geological Society, London.
- Peltier, W. R. (2002). On eustatic sea level history: Last Glacial Maximum to Holocene. *Quaternary Science Reviews* **21**, 377–396.
- Pirazzoli, P. A. (1991). *World Atlas of Holocene Sea-Level Changes*, Oceanography Series 58, p. 300. Elsevier, Amsterdam.
- Pirazzoli, P. A. (1996). *Sea-Level Changes: The Last 20 000 Years*, p. 211. John Wiley and Sons, Chichester.
- Ryan, W., and Pitman, W. (1998). *Noah's Flood: the new scientific discoveries about the event that changed history*, p. 319. Simon and Schuster, New York.
- Shennan, I. (1999). Global meltwater discharge and the deglacial sea-level record from northwest Scotland. *Journal of Quaternary Science* **14**, 715–719.
- Thom, B. G., and Chappell, J. (1975). Holocene sea levels relative to Australia. *Search* **6**, 90–93.
- Thom, B. G., and Roy, P. S. (1985). Relative sea levels and coastal sedimentation in southeast Australia in the Holocene. *Journal of Sedimentary Petrology* **55**, 257–264.
- Van Andel, T. H., and Veevers, J. J. (1967). Morphology and sediments of the Timor Sea. *Bulletin of the Bureau of Mineral Resources, Geology and Geophysics, Australia* **83**, 1–173.
- Veeh, H. H., and Veevers, J. J. (1970). Sea level at –175 m off the Great Barrier Reef 13,600 to 17,000 years ago. *Nature* **226**, 536–537.
- Yokoyama, Y., De Deckker, P., Lambeck, K., Johnston, P., and Fifield, L. K. (2001). Sea-level at the Last Glacial Maximum: evidence from northwestern Australia to constrain ice volumes for oxygen isotope stage 2. *Palaeogeography, Palaeoclimatology, Palaeoecology* **165**, 281–297.

Isostasy

G Milne and I Shennan, Durham University, Durham, UK

© 2007 Elsevier B.V. All rights reserved.

Introduction

Relative sea level (RSL) is defined as the height of the ocean surface relative to the solid Earth (or ocean floor) and can be defined at any location within the oceans. Changes in RSL are driven, therefore, by processes that produce a height shift in either of these two bounding surfaces. At any given location, RSL changes over a wide range of timescales with characteristic periods ranging from less than a second to millions of years. This broad spectrum of time variation reflects the variety of processes that drive RSL changes: atmospheric circulation, ocean circulation, changes in the distribution of grounded ice, lunar tides, deformation of the solid Earth associated with internal buoyancy forces (mantle convection), and changes in the distribution of mass at the Earth's surface (e.g., growth and melting of ice sheets, erosion, and deposition of rocks).

During the Quaternary, the dominant component of the RSL change observed using proxy records was driven by the accumulation and ablation of major ice sheets. There are a number of physical mechanisms associated with this glaciation-induced sea-level change and these are described in the following section. Models that incorporate these mechanisms can be employed to predict RSL changes, which can, in turn, be compared to the observations. It is through this modeling procedure that researchers have been able to better understand the physical processes involved in driving sea-level changes as well as place constraints on key model parameters. The most common applications of this type will be presented in the section 'Applications of Sea-Level Models.'

Physical Principles of Glaciation-Induced Sea-Level Change

Vertical Deflection of the Solid Earth

The late Quaternary ice sheets reached thicknesses of several kilometers in places. During a typical glacial cycle the net flux of mass from the oceans to the ice sheets and back again is on the order of 100 m of mean global sea-level change. This redistribution of surface water mass is large enough to cause a significant isostatic deformation of the solid Earth. This deformation is one of the important processes that contributes to glaciation-induced sea-level change (e.g., O'Connell (1971), Chappell (1974), Peltier and Andrews, (1976), and Clark *et al.* (1978)).

Figure 1 shows a model prediction of vertical deformation at present associated with the most recent deglaciation (ca. 20–7 cal kyr BP). The signal is dominated by crustal uplift in regions where large ice sheets once existed (e.g., North America, northwest Europe) or where the extent and thickness of ice was larger than at present (e.g., Antarctica). Even though ice had disappeared in North America and northwest Europe during the early- to mid-Holocene, there remains significant uplift in these regions due to the relatively high viscosity of mantle material, which limits the rate at which the solid Earth can attain isostatic equilibrium following the removal of ice. Note that there are extensive regions of subsidence peripheral to areas of uplift. This deformation is linked to uplift of the solid Earth in regions peripheral to the growing ice sheets; when the ice sheets

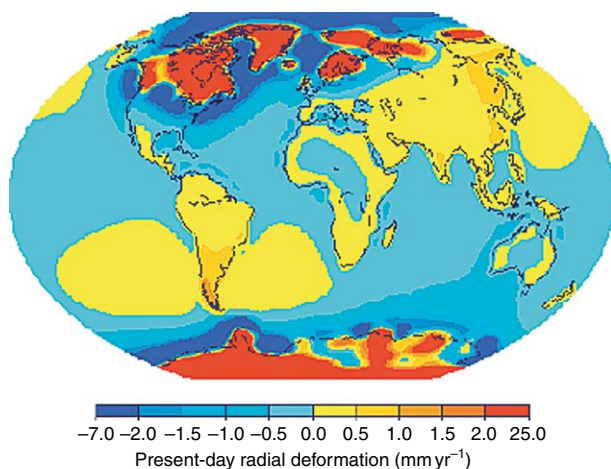


Figure 1 Predicted present-day vertical motion of the solid Earth based on a model of glacial isostatic adjustment. The ice component of the model is adapted from the ICE-3G deglaciation history (Tushingham and Peltier, 1991). Reproduced with permission from Pugh D (2004) *Changing Sea Levels: Effects of Tides, Weather and Climate*, p. 280. Cambridge: Cambridge University Press.

deglaciate, this process is reversed and these so-called 'peripheral bulges' subside.

The solid Earth deformation associated with the ice sheets, known as glacioisostasy, is by far the dominant signal in regions near major ice centers (so-called 'near-field' regions). A significant amount of deformation is also caused by the change in sea level associated with the change in ice distribution. The solid Earth deformation associated with this ocean loading, known as hydroisostasy, is most apparent in regions far from the major ice centers (so-called 'far-field' regions) where the glacioisostatic signal is considerably reduced. For example, the small uplift around the periphery of Australia and Africa in Figure 1 is associated with the positive ocean load applied around these continents during deglaciation. This uplift has been termed 'continental levering' (e.g., Clark *et al.* (1978)).

The surface mass redistribution and subsequent solid Earth deformation associated with Earth glaciation perturbs the Earth's inertia tensor and therefore affects a change in Earth rotation: commonly described as a change in the spin rate (change in length of day) and a change in the orientation of the spin axis relative to the solid Earth (True Polar Wander) (e.g., Sabadini *et al.* (1982) and Mitrovica *et al.* (2005)). The latter of these produces a significant global-scale deformation of the Earth due to the corresponding shift in the rotational potential. The dominant geometry of this deformation is shown in Figure 2. This rotation-induced pattern of deformation is relatively small (approximately 1–2 orders of

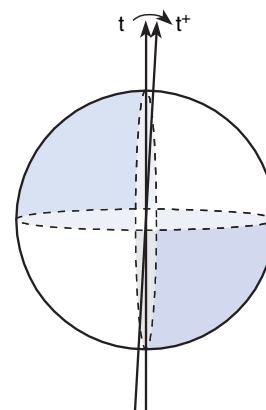


Figure 2 Schematic diagram illustrating the geometry of the vertical solid Earth deformation driven by a clockwise wander of the rotation pole between the times t and t^+ . Shaded areas indicate uplift and nonshaded areas indicate subsidence (associated with positive and negative perturbations to the rotational potential). Reproduced with permission from Mound JE and Mitrovica JX (1998) True Polar Wander as a mechanism for second-order sea-level variations. *Science* 279: 534–537.

magnitude less than the glacioisostatic signal). However, it is evident in [Figure 1](#) as broad regions of uplift centered on South America and northwest Asia and broad regions of subsidence centered on North America and Australia (the North American component of the signal is masked by the much larger glacioisostatic deformation).

Vertical Deflection of the Ocean Surface

As discussed above, the ocean surface is perturbed due to a variety of processes (winds, ocean circulation, tides, etc.). Over timescales of hundreds to thousands of years, the mean height of the ocean surface approximates the geodetic surface known as the geoid, which is an equipotential of the Earth's gravitational field. Therefore, for the purposes of modeling secular sea-level change associated with Earth

glaciation, vertical deflections of the ocean surface are determined by considering changes in the Earth's gravity field (or geopotential).

Any redistribution of mass on or within the Earth will affect the geopotential and therefore perturb the ocean surface. The height shift in the ocean surface caused directly by the flux of mass on the Earth's surface between ice sheets and oceans during glaciations and the changing rotational potential is known as the 'direct effect' (e.g., [Clark *et al.* \(1978\)](#)). The direct effect associated with an ablating ice sheet is illustrated schematically in [Figure 3](#). Between the two time steps t_0 and t_1 , the ice sheet loses mass and therefore the gravitational pull of the ice on the ocean water relaxes, causing a lowering of the ocean surface proximal to the ice and a height increase of the ocean surface in the far field. Note

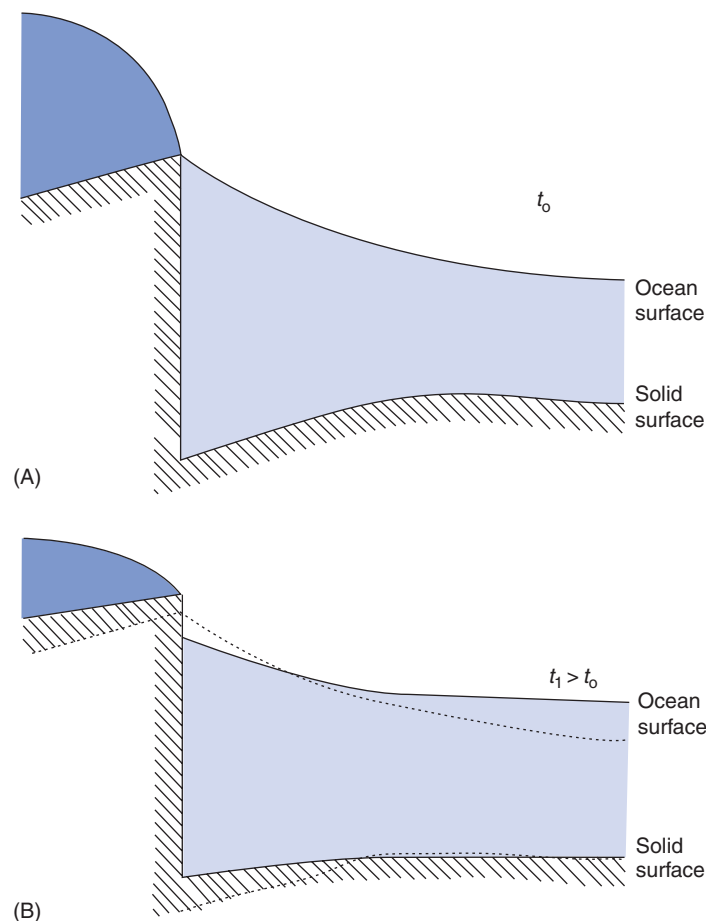


Figure 3 Schematic diagram illustrating the influence of an ablating ice sheet on the vertical displacement of the solid surface and the time-averaged ocean surface. The dotted lines in (B) denote the position of these two surfaces in (A). The difference between the solid and dotted lines in (B) illustrates the uplift of the solid Earth immediately under the ablating ice mass and the subsidence of the solid Earth peripheral to the ice mass; they also show the height shift of the ocean surface associated with the ice–ocean mass flux. This flux directly perturbs the geopotential causing the ocean surface to undergo a net fall near the ice mass and a net rise at a greater distance from the ice mass. Reproduced with permission from Tamisiea ME, Mitrovica JX, Davis JL, and Milne GA (2003) Long wavelength sea level and solid surface perturbation driven by polar ice mass variations: Fingerprinting Greenland and Antarctic ice sheet flux. *Space Science Reviews* 108: 81–93.

that the redistribution of ocean water has a similar effect – for example, regions characterized by a sea-level rise will experience a greater rise due to the increased gravitational pull of the deeper water column.

The perturbation to the geopotential due to the deformation of the solid Earth by the surface ice–ocean loading and changing rotational potential is termed the ‘indirect effect’ since it is a consequence of the solid Earth response to these changes. The spatial pattern of the sea-surface height change as a consequence of the indirect effect reflects that shown in **Figure 1**. For example, the mass influx of solid Earth material to uplifting regions causes an increase in the local geopotential and therefore produces a rise in the ocean surface.

Mass Conservation

An important criterion that must be satisfied when calculating sea-level change associated with the growth and ablation of ice sheets is that the mass lost (gained) by the ice sheets is gained (lost) by the oceans to ensure that the total amount of water within the system is conserved. This criterion is satisfied by ensuring that

$$\int_{\text{ocean}} S(\theta, \phi, t) dA = V_{\text{OW}}(t) = -\frac{\rho_i}{\rho_w} V_I(t) \quad [1]$$

in which $S(\theta, \phi, t)$ is the change in sea level since a reference time (e.g., the onset of glacial growth); $V_{\text{OW}}(t)$ and $V_I(t)$ are, respectively, the changes in the volume of ocean water and ice since the reference time; and ρ_i and ρ_w are the densities of ice and water, respectively. In most cases, to satisfy Eqn [1], a correction term is applied to the predicted sea-level change that corresponds to a spatially uniform height shift of the ocean surface (e.g., **Farrell and Clark (1976)** and **Mitrovica and Peltier (1991)**). This shift can be thought of as acting to change the equipotential that the mean ocean surface lies on during Earth glaciation. This shift is affected by two processes: the change in ocean water volume associated with ice-sheet growth/melting and the volumetric change in the height shift between the ocean surface and the ocean floor due to the processes described in the previous two subsections. In the former case, for example, the increase in ocean water volume during deglaciation will cause the ocean surface to rise, on average, and therefore lie on an equipotential further displaced from the Earth’s center. The second of these two processes leads to the mechanism known as ‘ocean syphoning’ (**Mitrovica and Peltier, 1991**).

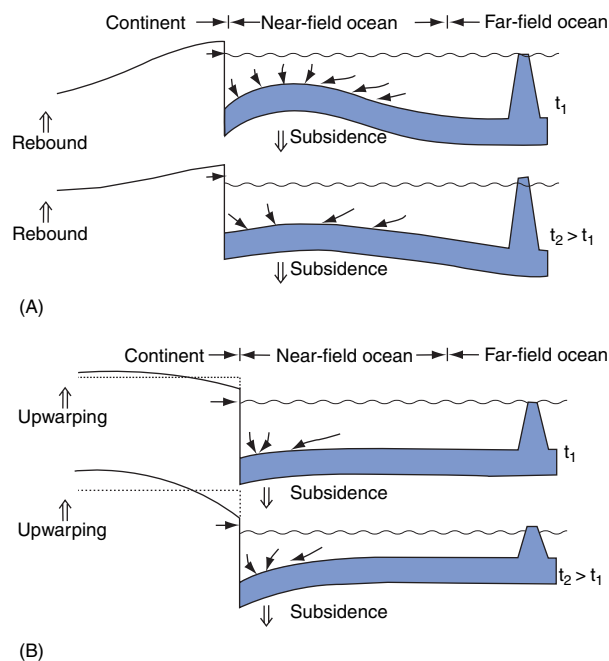


Figure 4 Schematic diagram illustrating the syphoning mechanism. (A) shows the lowering of the ocean surface caused by the syphoning of ocean water into subsiding peripheral bulge regions during periods of deglaciation. (B) illustrates the similar effect caused by subsidence around continental margins due to hydroisostasy during periods of deglaciation. Reproduced with permission from Mitrovica JX and Milne GA (2002) On the origin of late Holocene highstands within equatorial ocean basins. *Quaternary Science Reviews* 21: 2179–2190.

Ocean syphoning is driven by two aspects of glaciation-induced sea-level change – these are illustrated in **Figure 4**. **Figure 4A** shows the contribution to syphoning associated with peripheral bulge subsidence. A dominant proportion of peripheral bulges is located in oceanic regions and so the subsidence of these regions during deglaciation contributes to a significant, spatially uniform fall in sea level, as water is syphoned into these subsiding regions. **Figure 4B** illustrates the contribution of continental levering to the syphoning process during deglaciation (again, giving a sea-level fall). In total, the magnitude of the global mean sea-level fall due to syphoning during deglaciation is about 20–30 m from the Last Glacial Maximum (LGM) to present and is about 0.3 mm yr^{-1} at present (the magnitude of the signal depends on the rate of solid Earth motion which is governed by the Earth’s internal viscosity structure).

Sea-Level Equation

All of the above-described processes can be represented in a single equation that can be solved to predict sea-level change over the world’s oceans due

to Earth glaciation. Farrell and Clark, (1976) were the first to present and solve a version of the sea-level equation. Since their seminal work, a number of extensions have been made to the theory built into the equation as well as the methods applied to solve it. Solving the sea-level equation is nontrivial since the quantity being solved for is a key component of the surface load that drives the system. Most of the methods applied involve an iterative procedure and the most popular of these is the so-called ‘pseudospectral technique’ described by Mitrovica and Peltier, (1991).

The primary theoretical extensions to the original theory of Farrell and Clark, (1976) include the incorporation of shoreline migration, the influence of changes in Earth rotation, and a more accurate treatment of sea-level change in regions with ablating marine-based ice (see Milne (2002) for a review). The most recent form of the sea-level equation that incorporates all of these recent improvements in an accurate, generalized theory was published by Mitrovica and Milne, (2003) and can be solved efficiently by an algorithm that is based on the pseudospectral method (Kendall *et al.*, 2005).

Applications of Sea-Level Models

Introduction

The principal components of a model required to predict glaciation-induced sea-level change are shown in Figure 5. The two primary inputs to such a model are a reconstruction of global ice extent (geographic and thickness) throughout the period of interest and an Earth model to simulate the deformation associated with the surface load and rotational potential. Once these two inputs are prescribed, the sea-level equation can be solved, in conjunction with the Euler equations, to calculate the ocean component of the load and the rotational potential.

With all of these elements in place, the model can be applied to predict a number of geophysical observables associated with Earth glaciation: sea-level changes, present-day 3-D motion of the Earth’s

surface, present-day changes in the geopotential and the rotation vector (such as True Polar Wander). The term ‘glacial isostatic adjustment’ (GIA) is commonly applied to describe research that considers the isostatic response of the solid Earth to glaciation through modeling one or more of these observables (e.g., Peltier and Andrews, (1976)).

The sea-level equation and the physical mechanisms that can be incorporated within it were discussed in the previous section. The primary aim of this section is to describe how the Earth and ice models are constructed and then tested by comparing model predictions to sea-level observations, and some of the issues involved in doing this accurately.

Inferring Earth Viscosity Structure

The isostatic response of the solid Earth, for a given load history, is governed by its internal density and rheological structure. To a first approximation, this structure is spherically symmetric (i.e., is depth dependent only) and so the majority of Earth models previously employed for this purpose have not incorporated lateral variations in these properties. The rheological model applied most commonly is that of a Maxwell viscoelastic material, which simulates both an elastic and (linear) viscous component of the deformation. It is important to include an elastic component given that ice sheets can change dramatically within a relatively short time – a few hundred to a few thousand years.

The elastic and density structure of Earth models applied to problems of glaciation-induced sea-level change is taken from seismic constraints, whereas the viscosity structure is one of the parameters that can be inferred when modeling GIA datasets such as relative sea-level change. The viscosity structure of the deep Earth is a primary control on a number of geodynamic processes, including mantle convection, and there are a limited number of methods that can be applied to infer this structure (e.g., Ranalli (1995)). This application of the model is therefore one of the more important elements in sea-level modeling studies (e.g., Cathles (1975), Peltier (1998), and Lambeck and Johnston (1998)).

The viscosity structure in spherically symmetric Earth models is parametrized into a small number of layers. The most common parametrization comprises three layers. The lithosphere, the upper layer, is given a very large viscosity (10^{30} – 10^{50} Pa s), so that it behaves as an elastic layer on late Quaternary time-scales – the thickness of this layer is the variable parameter. The second layer extends from the base

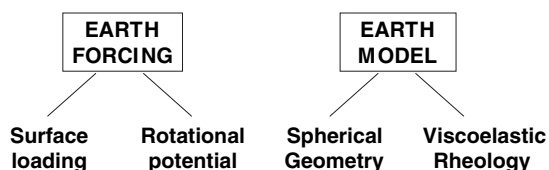


Figure 5 Schematic diagram illustrating the main components comprising a model of glacial isostatic adjustment.

of the model lithosphere to the 670 km deep seismic velocity discontinuity, and the third layer extends from this depth to the core–mantle boundary. These two layers represent the model upper and lower mantle, respectively, and are each assigned a single viscosity value that is a free parameter in the model. Note that a number of studies have considered other depth parametrizations (e.g., Lambeck *et al.* (1996)) and inverse modeling studies commonly parametrize viscosity into a much larger number of layers beneath the lithosphere (e.g., Forte and Mitrovia (1996) and Peltier (1998)).

As indicated in **Figure 1**, the largest magnitude of solid Earth deformation is found in areas that have experienced the largest changes in ice extent (e.g., North America, Fennoscandia). For this reason, sea-level observations from regions such as these have been most commonly adopted to infer viscosity structure. One primary limitation of modeling near-field data is that the model predictions are sensitive to both viscosity structure and the ice history. The accuracy of the viscosity inference will depend on the accuracy of the ice model (see the section ‘Inferring late Quaternary ice histories’). This ambiguity can be addressed to some extent by simultaneously modeling for both the ice history and the viscosity structure and performing sensitivity studies to determine the degree of parameter tradeoff between these two components of the model (e.g., Lambeck *et al.* (1998)).

An alternative way of addressing this issue of non-uniqueness involves identifying a parametrization or subset of the data that is relatively insensitive to one of either the viscosity model or ice model. Two parametrizations of near-field sea-level data that have been shown to reduce the sensitivity of the predictions to the ice history are the ‘decay-time’ parametrization (Mitrovia and Peltier, 1993) and the ‘relaxation spectrum’ derived from mapping out the elevation of ancient shorelines in Fennoscandia (McConnell, 1968).

A third approach to reducing the sensitivity of the data to uncertainty in the ice component of the model involves the application of far-field data. By definition, these observations are obtained in areas distant from the major glaciation centers and so the glacio-isostatic signal will be relatively small. However, the observations are sensitive to the ice model, largely through mass flux between the ice sheets and the oceans. This component of the signal has a very long wavelength and so by taking the difference between observations from distinct localities that correspond to the same time, one effectively removes any dependence on ice model parameters and so isolates the signal associated with hydroisostasy. This

parametrization of far-field data was pioneered by Nakada and Lambeck, (1989) who modeled differential Holocene highstand observations from the Australian region to obtain a robust inference of Earth viscosity structure.

Most inferences of Earth viscosity structure have been based on forward modeling analyses. However, the information obtained from the application of inverse methods has played an important role in partly reconciling the differences in inferences made by various groups (Mitrovia, 1996). Specifically, the explicit consideration of depth-resolving power in inverse analyses has clearly identified how well a particular set of sea-level data can constrain the depth variation of viscosity. Analyses of this type have shown that the depth-resolving power of a given sea-level data set depends on the spatial extent of the local ice sheet and the viscosity structure within the mantle (e.g., Mitrovia (1996)). The relatively small number of inverse modeling studies performed to date have shown that sublithosphere viscosity structure can be uniquely resolved in only 2–3 layers for any specific regional data set, with a maximum depth constraint extending to ~1,800 km for data associated with the deglaciation of the Laurentide Ice Sheet (e.g., Mitrovia (1996)).

The limited resolving power of sea-level data has been addressed by inverting these data jointly with other GIA data sets (e.g., Kaufmann and Lambeck (2002)) and data related to convective flow within the mantle (e.g., the global free air gravity anomaly, motion of the tectonic plates; Forte and Mitrovia (1996) and Mitrovia and Forte (2004)). With regard to the viscosity constraint provided by RSL observations, an optimal resolving power would be obtained by jointly modeling data from regions once covered by ice sheets with different geographic extent (e.g., the British Isles, Fennoscandia, and North America).

The real Earth is known to exhibit significant departures from spherical symmetry. With dramatic improvements in computational power, a growing number of groups have begun to model sea-level changes on global 3-D Earth models (e.g., Paulson *et al.* (2005) and Wu *et al.* (2005)). A primary aim of these studies has been to determine the significance of 3-D structure in predicting sea-level changes in order to assess the extent to which inferences of viscosity and ice histories (see the section ‘Inferring late Quaternary ice histories’) based on 1-D Earth models might have been biased.

A second important initiative with respect to modeling the isostatic component of the Earth response has been the consideration of rheologies

that incorporate transient creep (e.g., *Peltier et al. (1981)*) or nonlinear viscous flow (e.g., *Wu (1999)*). A large number of studies on the deformation of rocks and minerals at high pressures and temperatures in the laboratory have shown that, under a wide range of conditions, mantle rocks will deform in a nonlinear, power law fashion (e.g., *Drury and Fitzgerald (1998)*). It is expected that linear and nonlinear viscous flow will dominate in different parts of the sublithospheric mantle. The consideration of lateral variations in Earth model structure and more sophisticated (non-Maxwell) rheologies increases the level of complexity within GIA sea-level models and therefore the degree of nonuniqueness in obtaining model solutions. It remains to be seen just how large an impact these developments will have in this regard.

Inferring Late Quaternary Ice Histories

A second important application of sea-level modeling is the inference of more accurate ice-sheet reconstructions – particularly for the period following the LGM during which there is a relative abundance of high-quality RSL data. As indicated in *Figure 5*, constraining the evolution of the Earth's ice sheets during the late Quaternary is addressed via a number of different research disciplines, most notably: glacial geology, glaciology, and GIA.

The strong impact of ice sheets on other components of the climate system has become evident through the application of general circulation models of climate change, in which reconstructions of ice-sheet evolution are input as a boundary condition. A continued effort to employ RSL observations to better constrain such reconstructions is clearly important for this reason and these constraints will complement information derived from glaciological observations and modeling as well as field-based geological and geophysical studies.

As discussed in the previous subsection, near-field sea-level data can be employed to develop regional and global reconstructions of ice sheets (e.g., *Tushingham and Peltier (1991)*, *Lambeck (1993)*, and *Lambeck et al. (1998)*). The veracity of these models depends largely on the quality of the data employed in their construction (sea level and other), the introduction of biases due to tradeoffs between earth and ice model parameters, and the magnitude of any inaccuracies in the modeled Earth response. As discussed in the previous subsection, an efficient way in which to reduce the ambiguity due to parameter tradeoff is to identify parametrizations or subsets of the data that are relatively insensitive to either the Earth or ice component of the model. For

example, employing a viscosity model that is based on the decay time parametrization (which is relatively insensitive to the ice loading model; see previous subsection) to derive an ice-sheet reconstruction would be an efficient way to minimize the nonuniqueness problem inherent within near-field sea-level data.

Due to their distance from the major glaciation centers, far-field RSL data exhibit a primary sensitivity to mass flux between the ice sheets and oceans. For this reason, when the data are corrected for the processes that cause the signal to deviate from the eustatic signal (due to glacio- and hydroisostasy, syphoning, etc.; see previous section), they provide a useful measure of the total volume of grounded ice on the Earth's surface in the past compared to the present, which can be compared to, or used to calibrate, ice-volume estimates based on oxygen isotope records. Estimates of LGM ice volume have converged within the past few years and generally lie within the range of 120–135 m of equivalent (eustatic) sea-level change (e.g., *Lambeck et al. (2002)*, *Milne et al. (2002)*, and *Peltier (2004)*). These estimates serve as an important constraint to which global LGM ice-sheet reconstructions must adhere to. Note that, the most recent estimates of this volume strongly support the CLIMAP 'minimum model' with 127 m of ice-equivalent sea level lowering compared to the 'maximum model' with 163 m of eustatic change (*CLIMAP, 1981*).

The modeling of post-LGM far-field RSL data has greatly enhanced our understanding of the rate and sources of glacial melting from the LGM to the present. Far-field observations have been interpreted to support the existence of a series of very rapid and short-lived melting events during the most recent deglaciation. For example, from the LGM to the Lateglacial, three such events have been proposed:

- ~19 cal kyr BP (10–15 m; *Yokoyama et al. (2000)*);
- ~14 cal kyr BP (20–30 m; *Fairbanks (1989)*, *Bard et al. (1990)*, and *Hanebuth et al. (2000)*); and
- ~11.5 cal kyr BP (10–15 m; *Fairbanks (1989)* and *Bard et al. (1990)*).

Determining how these meltwater pulses relate to other large and rapid climate events during this period is central to our understanding of deglacial- and millennial-scale climate change. A necessary first step toward this aim involves determining which ice reservoirs were the primary contributors to these events.

In far-field locations, the direct gravitational effect of ice-sheet ablation (see *Fig. 4* and related discussion) is the mechanism that dominates the spatial

variation in the predicted sea-level signal during rapid melt events. The contribution from solid Earth isostatic deformation is relatively minor and so, given an appropriate spatial distribution of data that capture a specific melt event, it is possible to obtain relatively robust constraints on the global-scale source geometry for that event. The first studies of this kind have shown, for example, that the existing far-field data favor a dominant Antarctic rather than North American source for the ~14 cal kyr BP event termed 'meltwater pulse IA' (Clark *et al.*, 2002; Bassett *et al.*, 2005). This melt source model can be tested further and spatially refined by modeling near-field sea-level data from Antarctica. If proven correct, this result will have important implications for our understanding of climate system evolution during Termination 1 (Weaver *et al.*, 2003).

A number of far-field RSL observations display a high stand during the early- to mid-Holocene. Sea-level modeling has shown that this high stand results from a dramatic decrease in the rate of glacial melting around this time, which leads to the subsequent sea-level fall through the operation of ongoing isostatic effects, primarily syphoning and hydroisostasy (e.g., Clark *et al.* (1978) and Mitrovica and Peltier (1991)). The shape (e.g., smooth or sharp), timing, and magnitude of these high stands are controlled by both the isostatic response of the solid Earth and the rate and magnitude of glacial melting. The isostatic component can be effectively isolated and therefore modeled by considering spatial differences in the observed sea-level high stands (Nakada and Lambeck (1989); see previous section). The solid Earth component can then be predicted and removed from the observations, leaving a residual signal that provides a direct measure of when and how abruptly the most recent deglaciation ended and the history of global-scale melting after this time (e.g., Fleming (1998) and Peltier (2002)). The latter serves as an important reference value with which to compare estimates of global mean sea-level rise during the twentieth century (e.g., Lambeck (2002)).

Summary

Changes in RSL during the Quaternary are dominated by large-scale glaciation. A number of physical mechanisms contribute to glaciation-induced sea-level changes through their influence on the relative vertical height between the ocean floor and the ocean surface. These physical mechanisms provide the theoretical basis of the so-called sea-level equation, which can be solved to generate predictions of glaciation-induced sea-level changes for a prescribed Earth and

ice model. These predictions can be compared to observations to test the accuracy of the model and to infer model parameters. With respect to the Earth model, the majority of such studies have focused on inferring the viscosity structure within the mantle. This structure is a primary control on a variety of geodynamic processes that involve the viscous flow of mantle material. With respect to the ice model, the majority of such studies have focused on inferring the space-time history of regional-scale ice extent as well as the time variation in global (grounded) ice volume, during and following the LGM. This information has played a key role in advancing our understanding of ice age climate change.

See also: **Sea Level Studies:** Overview; Geomorphological Indicators; Low Energy Coasts Sedimentary Indicators; Coral Records; Eustatic Sea-Level Changes Since the Last Glaciation. **Sea-Levels, Late Quaternary:** High Latitudes; Mid-Latitudes; Tropics.

References

- Bard, E., Hamelin, B., Fairbanks, R. G., and Zindler, A. (1990). Calibration of the 14C timescale over the past 30,000 years using mass spectrometric U–Th ages from Barbados corals. *Nature* **345**, 405–410.
- Bassett, S. E., Milne, G. A., Mitrovica, J. X., and Clark, P. U. (2005). Ice sheet and solid earth influences on far-field sea-level histories. *Science* **309**, 925–928.
- Cathles, L. M. (1975). *The Viscosity of the Earth's Mantle*. p. 386. Princeton University Press, Princeton.
- Chappell, J. (1974). Late Quaternary glacio- and hydro-isostasy, on a layered earth. *Quaternary Research* **4**, 429–440.
- Clark, J. A., Farrell, W. E., and Peltier, W. R. (1978). Global changes in postglacial sea level: A numerical calculation. *Quaternary Research* **9**, 265–287.
- Clark, P. U., Mitrovica, J. X., Milne, G. A., and Tamisiea, M. (2002). Sea-level fingerprinting as a direct test for the source of global meltwater pulse 1A. *Science* **295**, 2438–2441.
- CLIMAP (1981). Seasonal reconstruction of the Earth's surface at the Last Glacial Maximum. *Geological Society of America, Map and Chart Series MC-36*.
- Drury, M. R., and Fitzgerald, J. D. (1998). Mantle rheology: Insights from laboratory studies of deformation and phase transition. In *The Earth's Mantle: Composition, Structure and Evolution* (I. Jackson, Ed.), pp. 503–560. Cambridge University Press, Cambridge.
- Fairbanks, R. G. (1989). A 17000-year glacio-eustatic sea level record: Influence of glacial melting rates on the Younger Dryas event and deep-ocean circulation. *Nature* **342**, 637–642.
- Farrell, W. E., and Clark, J. A. (1976). On postglacial sea-level. *Geophysical Journal of the Royal Astronomical Society* **46**, 647–667.
- Fleming, K., Johnston, P., Zwartz, D., Yokoyama, Y., Lambeck, K., and Chappell, J. (1998). Refining the eustatic sea-level curve since the Last Glacial Maximum using far- and intermediate-field sites. *Earth and Planetary Science Letters* **163**, 327–342.
- Forte, A. M., and Mitrovica, J. X. (1996). A new inference of mantle viscosity based on a joint inversion of post-glacial

- rebound data and long-wavelength geoid anomalies. *Geophysical Research Letters* **23**, 1147–1150.
- Hanebuth, T., Statterger, K., and Grootes, P. M. (2000). Rapid flooding of the Sunda Shelf: A late-glacial sea-level record. *Science* **288**, 1033–1035.
- Kaufmann, G., and Lambeck, K. (2002). Glacial isostatic adjustment and the radial viscosity profile from inverse modelling. *Journal of Geophysical Research* **107**, doi:10.1029/2001JB000941.
- Kendall, R., Mitrovia, J. X., and Milne, G. A. (2005). On post-glacial sea level. II: Numerical formulation and comparative results on spherically symmetric models. *Geophysical Journal International* **161**, 679–706.
- Lambeck, K. (1993). Glacial rebound of the British Isles. II: A high resolution, high-precision model. *Geophysical Journal International* **115**, 960–990.
- Lambeck, K. (2002). Sea level change from mid-Holocene to recent time: An Australian example with global implications. In *Glacial Isostatic Adjustment and the Earth System: Sea Level, Crustal Deformation, Gravity and Rotation*, AGU monograph, *Geodynamics Series* 29 (J. X. Mitrovia and L. L. A. Vermeersen, Eds.), pp. 33–50. AGU, Washington DC, USA.
- Lambeck, K., and Johnston, P. (1998). The viscosity of the mantle: Evidence from analyses of glacial-rebound phenomenon. In *The Earth's Mantle: Composition, Structure and Evolution* (I. Jackson, Ed.), pp. 461–502. Cambridge University Press, Cambridge.
- Lambeck, K., Johnston, P., Smither, C., and Nakada, M. (1996). Glacial rebound of the British Isles. III: Constraints on mantle viscosity. *Geophysical Journal International* **125**, 340–354.
- Lambeck, K., Smither, C., and Johnston, P. (1998). Sea-level change, glacial rebound and mantle viscosity for northern Europe. *Geophysical Journal International* **134**, 102–144.
- Lambeck, K., Yokoyama, Y., and Purcell, A. (2002). Into and out of the Last Glacial Maximum: sea-level change during oxygen isotope stages 3 and 2. *Quaternary Science Reviews* **21**, 343–360.
- McConnell, R. K. (1968). Viscosity of the mantle from relaxation time spectra of isostatic adjustment. *Journal of Geophysical Research* **73**, 7089–7105.
- Milne, G. A. (2002). Recent advances in predicting glaciation-induced sea-level changes and their impact on model applications. In *Glacial Isostatic Adjustment and the Earth System: Sea Level, Crustal Deformation, Gravity and Rotation*, AGU monograph, *Geodynamics Series* 29 (J. X. Mitrovia and L. L. A. Vermeersen, Eds.), pp. 157–176. AGU, Washington DC, USA.
- Milne, G. A., Mitrovia, J. X., and Schrag, D. P. (2002). Estimating past continental ice volume from sea-level data. *Quaternary Science Reviews* **21**, 361–376.
- Mitrovia, J. X. (1996). Haskell (1935) revisited. *Journal of Geophysical Research* **101**, 555–569.
- Mitrovia, J. X., and Forte, A. M. (2004). A new inference of mantle viscosity based upon joint inversion of convection and glacial isostatic adjustment data. *Earth and Planetary Science Letters* **225**, 177–189.
- Mitrovia, J. X., and Milne, G. A. (2002). On the origin of late Holocene highstands within equatorial ocean basins. *Quaternary Science Reviews* **21**, 2179–2190.
- Mitrovia, J. X., and Milne, G. A. (2003). On post-glacial sea level. I: General theory. *Geophysical Journal International* **154**, 253–267.
- Mitrovia, J. X., and Peltier, W. R. (1991). On post-glacial geoid subsidence over the equatorial oceans. *Journal of Geophysical Research* **96**, 20,053–20,071.
- Mitrovia, J. X., and Peltier, W. R. (1993). A new formalism for inferring mantle viscosity based on estimates of post glacial decay times: Application to RSL variations in N. E. Hudson Bay. *Geophysical Research Letters* **20**, 2183–2186.
- Mitrovia, J. X., Wahr, J., Matsuyama, I., and Paulson, A. (2005). The rotational stability of an ice-age earth. *Geophysical Journal International* **161**, 491–506.
- Mound, J. E., and Mitrovia, J. X. (1998). True Polar Wander as a mechanism for second-order sea-level variations. *Science* **279**, 534–537.
- Nakada, M., and Lambeck, K. (1989). Late Pleistocene and Holocene sea-level change in the Australian region and mantle rheology. *Geophysical Journal International* **96**, 497–517.
- O'Connell, R. J. (1971). Pleistocene glaciation and the viscosity of the lower mantle. *Geophysical Journal* **23**, 299–327.
- Paulson, A., Zhong, S., and Wahr, J. (2005). Modelling post-glacial rebound with lateral viscosity variations. *Geophysical Journal International* **163**, 357–371.
- Peltier, W. R. (1998). Postglacial variations in the level of the sea: Implications for climate dynamics and solid-earth geophysics. *Reviews of Geophysics* **36**, 603–689.
- Peltier, W. R. (2002). On eustatic sea level history: Last Glacial Maximum to Holocene. *Quaternary Science Reviews* **21**, 377–396.
- Peltier, W. R. (2004). Global glacial isostasy and the surface of the ice-age earth: The ICE-5G (VM2) model and GRACE. *Annual Review of Earth and Planetary Sciences* **32**, 111.
- Peltier, W. R., and Andrews, J. T. (1976). Glacial isostatic adjustment. I: The forward problem. *Geophysical Journal of the Royal Astronomical Society* **46**, 605–646.
- Peltier, W. R., Wu, P., and Yuen, D. A. (1981). The viscosities of the Earth's mantle. In *Anelasticity in the Earth*, AGU and GSA, *Geodynamics Series* 4 (F. D. Stacey, M. S. Paterson and A. Nicolas, Eds.), pp. 59–77. AGU, Washington DC, USA.
- Pugh, D. (2004). *Changing Sea Levels: Effects of Tides, Weather and Climate*. p. 280. Cambridge University Press, Cambridge.
- Ranalli, G. (1995). *Rheology of the Earth*, 2nd edn., p. 413. Chapman and Hall, London.
- Sabadini, R., Yuen, D. A., and Boschi, E. (1982). Polar wander and the forced responses of a rotating, multilayered, viscoelastic planet. *Journal of Geophysical Research* **87**, 2885–2903.
- Tamisiea, M. E., Mitrovia, J. X., Davis, J. L., and Milne, G. A. (2003). Long wavelength sea level and solid surface perturbation driven by polar ice mass variations: Fingerprinting Greenland and Antarctic ice sheet flux. *Space Science Reviews* **108**, 81–93.
- Tushingham, A. M., and Peltier, W. R. (1991). ICE-3G: A new global model of late Pleistocene deglaciation based on geophysical predictions of post-glacial relative sea level change. *Journal of Geophysical Research* **96**, 4497–4523.
- Weaver, A. J., Saenko, O. A., Clark, P. U., and Mitrovia, J. X. (2003). Meltwater Pulse 1A from Antarctica as a trigger of the Bølling-Allerød warm interval. *Science* **299**, 1709–1713.
- Wu, P. (1999). Modelling postglacial sea levels with power-law rheology and a realistic ice model in the absence of ambient tectonic stress. *Geophysical Journal International* **139**, 691–702.
- Wu, P., Wang, H., and Schotman, H. (2005). Postglacial induced surface motions, sea-levels and geoid rates on a spherical, self-gravitating laterally heterogeneous earth. *Journal of Geodynamics* **39**, 127–142.
- Yokoyama, Y., Lambeck, K., De Deckker, P., Johnston, P., and Fifield, L. K. (2000). Timing of the Last Glacial Maximum from observed sea-level minima. *Nature* **406**, 713–716.